A High Efficiency Class-E Power Amplifier with Tuned Output Network

Evan Court and Vipin Balyan
Department of Electrical, Electronics & Computer Engineering
Cape Peninsula University of Technology, Cape Town,
South Africa
evan.courtwp@gmail.com,vipin.balyan@rediffmail.com

2023 9th International Conference on Signal Processing and Communication (ICSC) | 979-8-3503-8320-1/23/$31.00 ©2023 IEEE | DOI: 10.1109/ICSC60394.2023.10441126

***Abstract*—A switch-mode power amplifier (PA), like the proposed class-E renders itself capable of achieving a theoretical power conversion efficiency (*PE*) of 100% by ensuring specific bias and switching conditions of the active device and presenting an idealized impedance at the drain of the active device [1] [2] [3]. The design presented satisfies the zero-voltage switching (ZVS) and zero derivative voltage switching (ZVDS) conditions which are fundamental to correct class-E PA operation. The output network performs a dual function of impedance transformation to a standard 50 ohm impedance and harmonic suppression for any power being transmitted at harmonic frequencies.**

***Keywords*—Class-E, transmission line, microstrip, GaN HEMT, power amplifier (PA), harmonic suppression, power efficiency (PE), power added efficiency (PAE).**

I. INTRODUCTION

Class E PAs and many variants thereof, have been proposed and developed with the objective of improving *PE* and increasing RF output power. Applicable to many switch-mode PAs and different classes, class E power amplifiers satisfy the necessary criteria for achieving a maximum theoretical *PE*[5]. Switching power amplifiers renders itself to the active device is operated as a switch. The conduction period and the switching regularity is determined by the duty-cycle of the active device, irrespective of the type of device implemented by the designer. Dependant on the wave-shaping technique implemented and the bias conditions of the active device, switching PAs can further be categorised into class D, E, F and inverse class F. The nonlinear operation of switching PAs is due to power in the harmonics at the output port being considerably increased in comparison to linear PAs. The nonlinear nature of switching PAs allow for superior *PE* and reduced signal bandwidth to be achieved[6].

The operation and performance of a PA can be defined and quantified by certain parameters. These parameters give us insight to the effectiveness of the amplification process relative to the power level of the input RF signal $P_{\mathrm{RF(in)}}$ .at a specific frequency, or within a frequency band, and is mathematically expressed as [3]

$$P_{\mathrm{RF(in)}}(f) = \frac{1}{2}\mathrm{Re}\left\{V_{\mathrm{in}} I_{\mathrm{in}}^{*}\right\} \quad \mathrm{W} \tag{1}$$

The output power of a PA, $P_{\mathrm{RF(out)}}$, is the power delivered to the external load and is expressed as

$$P_{\mathrm{RF(out)}}(f) = \frac{1}{2}\mathrm{Re}\left\{V_{\mathrm{out}} I_{\mathrm{out}}^{*}\right\} \quad \mathrm{W} \tag{2}$$

The power gain, which is a function of frequency, is expressed by equation (3) as [3] [4]

$$G(f) = \frac{P_{\mathrm{RF(out)}}(f)}{P_{\mathrm{RF(in)}}(f)} \tag{3}$$

The *PE* of PA is a measure of the total applied DC power converted into RF output power. Depending on the active device, it is also referred to as the drain or collector efficiency, respectively. The *PE* can be mathematically expressed as equation (4) [3] [5]

$$\eta = \frac{P_{\mathrm{RF(out)}}}{P_{\mathrm{DC}}} \times 100\% \tag{4}$$

For the linear region of the gain (i.e. where G remains constant and its magnitude is independent and unaffected by the magnitude of $P_{\mathrm{RF(in)}}$), there is an exponential increase in the efficiency of the PA for any increase in $P_{\mathrm{RF(in)}}$. However, due to the non-linear behaviour of any active device, there is a threshold where both G and P_{DC} are dependent on the magnitude of $P_{\mathrm{RF(in)}}$. At this stage we will start experiencing gain compression and the efficiency of the PA will start saturating [3]. Operating at microwave frequencies and above, a significant portion of the RF output power is directly as a result of the RF input power. For this reason, the RF input power, $P_{\mathrm{RF(in)}}$, cannot be neglected when determining the overall efficiency of a PA. The net increase in the total signal power of a PA, considering the RF input signal is mathematically expressed by equation (5) [6]

$$PAE = \frac{P_{\mathrm{add}}}{P_{\mathrm{DC}}} = \frac{P_{\mathrm{RF(out)}} - P_{\mathrm{RF(in)}}}{P_{\mathrm{DC}}} \tag{5}$$

Realizing a lossless amplifier requires some optimum and necessary conditions to exist. One such condition: $t=T$ is the time moment the switch closes, where T is the RF period. At this moment [2],

$$v_{\mathrm{DS}}(t)\big|_{t=T} = 0 \tag{6}$$

$v_{\mathrm{DS}}(t)$ being the drain-source voltage of the FET with respect to time. Another such condition:

$$\left.\frac{dv_{\mathrm{DS}}(t)}{dt}\right|_{t=T} = 0 \tag{7}$$

This implies that the drain-source capacitor has completely discharged and no increase in drain current will be experienced. We therefore establish a relationship between certain circuit parameters $(f_{max}, C \text{ and } V_{DD})$ in order to determine up to which frequency we can extend this operation. We start establishing such a relationship by substituting equation (8) into equation (9), which results in [7]

$$\omega CR = 0.1836 \tag{8}$$

$$\therefore\ R = \frac{0.1836}{\omega C}$$

$$I_0 = 0.5768\frac{V_{DD}}{R} \tag{9}$$

$$\therefore\ I_0 = \pi V_{DD}\omega C$$

An optimum class-E PA is limited to a maximum frequency of operation to realize such before degradation in efficiency is realized. Applying the device and circuit parameters for this study, we determine the maximum theoretical operating frequency for the selected active device.

$$f_{max} = \frac{1}{\pi^2}\frac{1}{\sqrt{\pi^2+4}+2}\frac{I_{max}}{C_{out}V_{DD}} \tag{10}$$

$$= \frac{I_{max}}{56.4995C_{out}V_{DD}}$$

An illustration of the proposed class-E is provided in Figure 1.

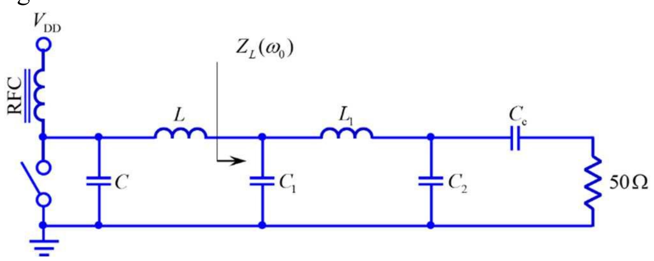

Figure 1: Class-E equivalent circuit

II. Circuit Analysis

The output network of the proposed class-E PA with shunt capacitance and series inductance is presented along with the design method. By applying the first condition to realize an ideal class-E operation, given by equation (12), we determine the phase angle as [1],

$$V_{max} = -2\pi\varphi V_{DD}\quad (\text{V}) \tag{11}$$

where,

$$\varphi = \tan^{-1}\left(\frac{-2}{\pi}\right) \tag{12}$$

$$= -0.5669 \text{ radians}$$

Thus,

$$V_{max} = 3.5619V_{DD} \tag{13}$$

and

$$I_{max} = \left(\frac{\sqrt{\pi^2+4}}{2}+1\right)I_0 \tag{14}$$

$$= 2.8621I_0$$

Now, considering the breakdown voltage of the active device $(V_{BR} = 120\text{ V})$, the maximum voltage will be limited to

$$V_{max} = 3.5619V_{DD}$$

$$\therefore\ V_{DD(max)} = \frac{120}{3.5619}$$

$$= 33.6899\text{ V}$$

Based on specific circuit parameters V_{DD} and $P_{RF(out)}$, we determine the optimum load impedance R as follows,

$$R = \frac{8}{\pi^2+4}.\frac{V_{DD}^{\ 2}}{P_{RF(out)}} \tag{15}$$

$$= 0.5768\frac{V_{DD}^{\ 2}}{P_{RF(out)}}$$

The optimum shunt capacitance C and series inductance L are determined using equations (16) and (17).

$$\frac{\omega L}{R} = \frac{V_L}{V_R} = 1.1525 \tag{16}$$

$$\omega CR = \frac{\omega C}{I_R}V_R = 0.1836 \tag{17}$$

We start designing the π-network by splitting the circuit into two back-to-back L-networks with aid of a virtual resistor, R_V, as illustrated in Figure 2 [8].

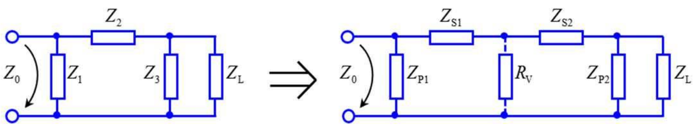

Figure 2: Splitting the pi-network

For a low-pass configuration, combining the two series inductive reactance values, the π-network can be represented as per Figure 3.

The output network is required to transform the optimum load impedance of 90.4422 Ω to the standard impedance of 50 Ω at the fundamental frequency and provide sufficient harmonic suppression at integer multiples of the fundamental frequency. A π-matching network is decided upon due to the high loaded Q (Q_L) requirement and three-element matching networks are suitable for high Q_L circuits, where $Q_L \geq 10$ [8].

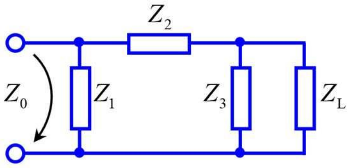

$$|Z_1| = 6.7522\,\Omega$$
$$|Z_2| = 15.5859\,\Omega$$
$$|Z_3| = 9.0442\,\Omega$$

Figure 3: Pi-network with relevant reactance values

Determining the component values from the corresponding reactance values calculated above, the equivalent class-E circuit can be realized and is illustrated in Figure 4.

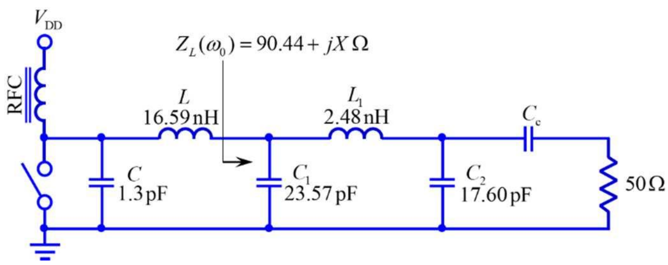

Figure 4: Realizable class-E amplifier

III. Simulation Results

The component values of the PA circuit are tuned using ADS optimiser such that the *PE* can be maximised at the fundamental frequency. Optimisation is also required as result of ideal lumped components behaving considerably different to real design models of the same component. An illustration of the PA schematic is provided in Figure 5, showing the tuned values of the components.

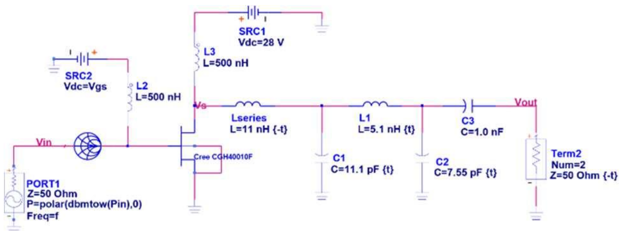

Figure 5: Lumped circuit schematic of designed class-E PA

The following step in the design procedure is to convert the lumped element circuit into a transmission-line equivalent.

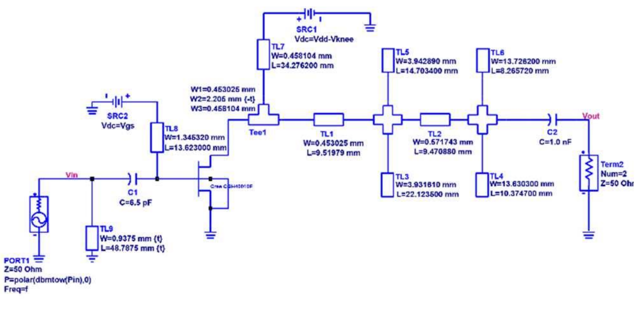

Figure 6: Transmission line equivalent class-E PA

The microstrip PA above was simulated without performing any optimization to the circuit. The circuit represents a direct transformation from the ideal transmission line PA to its microstrip equivalent. Optimization of the microstrip PA was implemented and the simulation of the design was performed yielding the results shown in Figure 7 to Figure 12. The PA performance is measured against the variation of the RF input power, $P_{RF(in)}$ at the fundamental frequency of 1 GHz. The DC bias conditions is set at $V_{DD} = 28\,\text{V}$ and $V_{GS} = -2.75\,\text{V}$.

The input and output return loss of the designed load is simulated by S-parameter simulation using Advanced Design Systems (ADS) by Agilent. The simulation is run over a frequency sweep from 0 - 5 GHz, illustrating the power transfer at the fundamental frequency. The simulation results show a good match between the optimum impedance presented to the output of the active device and the actual load impedance of 50 ohm.

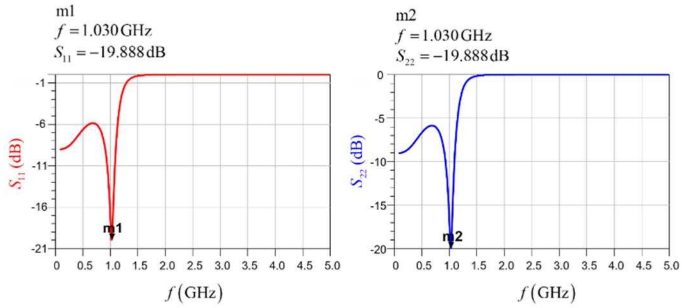

Figure 7: Input and output return loss of the load network

An S-parameter simulation was performed over a frequency range of 1-10 GHz. A plot of the simulation results as shown in Figure 8 illustrates the suppression of RF power at harmonic frequencies, thereby confirming operation of the output network. Significant attenuation is exhibited at even and odd harmonic frequencies, which is the desired result. This means minimal RF power is being delivered to the load at these frequencies. Equally important to note is that approximately 0 dB attenuation is experienced at the fundamental frequency of 1 GHz. This implies that maximum power will be delivered to the load at 1 GHz [9].

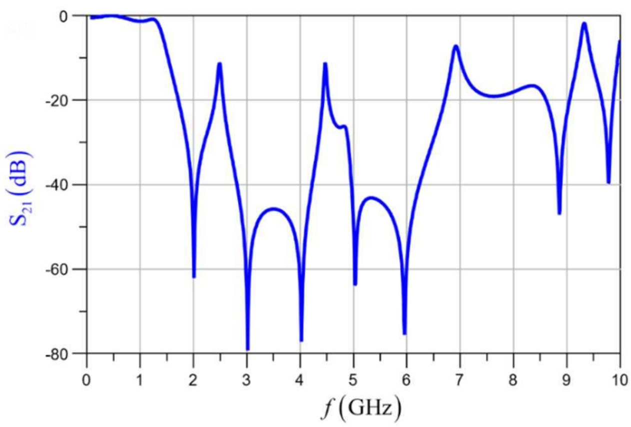

Figure 8: S_{21} response of the output network

The transient response of the drain voltage across the switch and drain current flowing through the switch is shown in Figure 9, illustrating the voltage being at a maximum magnitude when the drain current is near zero and the maximum drain current flowing when the drain voltage is at a minimum [1] [9].

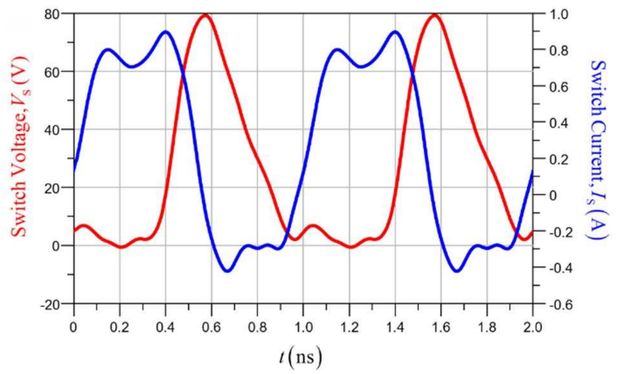

Figure 9: Drain voltage and current waveforms of optimized microstrip circuit.

The maximum RF output power, $P_{RF(out)}$ is measured at marker 3 as 39 dBm, shown in Figure 10. This is measured at $P_{RF(in)}$ of 35 dBm. It is important to note that despite the maximum output power being achieved at the input power level of 35 dBm, the maximum *PE* is achieved at $P_{RF(in)}$ 26 dBm. That is, 91% of the applied DC power is transformed into RF output power meaning only 9% is being dissipated or radiated as heat.

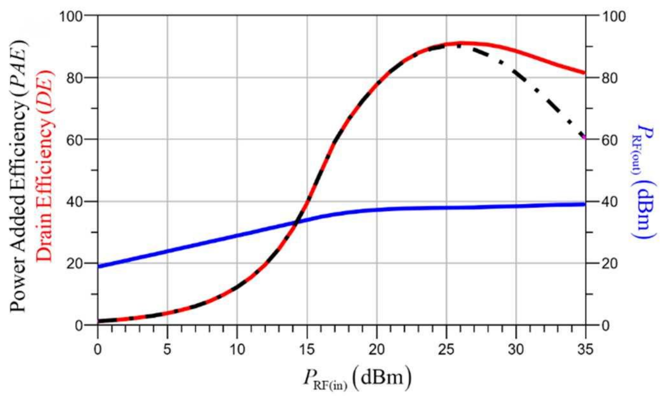

Figure 10: Simulated performance of PA with respect to input power

The optimized microstrip PA was measured against the drain supply voltage, V_{DD} subjecting the PA to conditions where any variations in the supply voltage may occur. This is a common scenario in CubeSats, which is the intended design objective. The results shown in Figure 11 signifies that this PA maintains a *PE* above 90% for V_{DD} swept from 15 V to 32 V. The *PAE* is maintained above 87% for the same simulation sweep of V_{DD}. This simulation is performed at the fundamental frequency of 1 GHz. A comparison is made with the performance of passed designs of high efficiency class-E PAs.

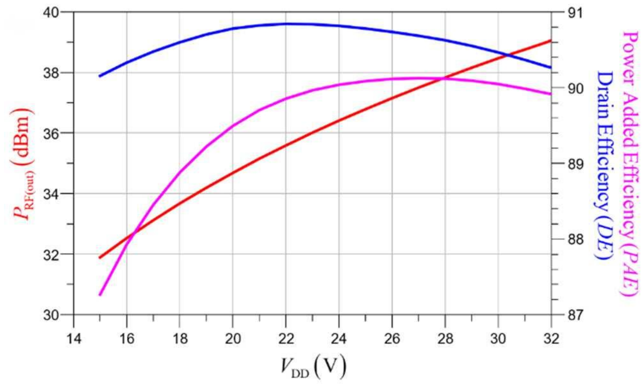

Figure 11: Simulated performance of PA with respect to DC supply voltage

The PAs instantaneous *PAE*, simulated at $V_{DD} = 28\,\text{V}$ is plotted in Figure 12 showing the degradation of the PAE at lower levels of RF output power. This simulation is done without the implementation of quasi-static envelope tracking, as employed by Mugisho *et al*. [2].

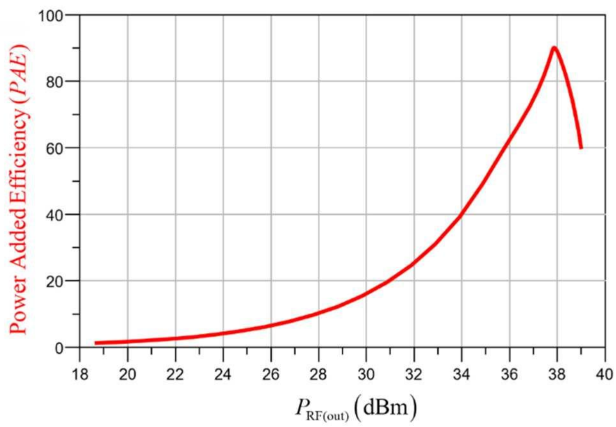

Figure 12: Simulated PAE with respect to output power

A comparison between the designed PA in this study is made to previously designed high efficiency class-E PAs. The performance of the various class-E designs are summarized in Table 1. The referenced PAs in Table 1 all implement a GaN HEMT as the active device, apart from [24] utilizing a GaAs PHEMT.

Ref	Freq (GHz)	(V)	*PE* (%)	*PAE* (%)	(dBm)	Gain (dB)
[20]	2	28	84.6	80.1	40.7	12.7
[21]	1.9	30	63	57	37	10
[22]	1.5	28	85	81	42	13.1
[5]	1.37	28	90.2	82.7	39.8	11.5
[23]	1	25	78.8	77.7	37	18.5
[24]	1	28	77.5	74.2	39.8	13.7
This work	1	28	91	90.3	37.89	11.8

Table 1: Comparison of Class-E Power Amplifiers

IV. Conlcusion

The proposed class-E PA employs a 50% duty-cycle of the GaN HEMT with shunt capacitance and a shunt ouput network. Derivation of the optimum parameters for the load network, switch voltage and switch current waveforms are included and verified through harmonic balance and frequency domain simulations. The mathematically derived parameter values and the simulation results correspond extremely well, fulfilling the conditions of ZVS and ZVDS required for class-E operation. The lumped component PA and TL class-E PA both exhibit a PE of 90%, however the TL equivalent required optimization and tuning due to the frequency response of lumped elements and TL being substantially different. Both PA circuits exhibit extremely good harmonic suppression, especially at first and second harmonic frequencies where majority of the harmonic power is being transmitted.

V. Acknowledgements

The authors extend a huge thank you to Wolfspeed for providing spice models and samples of the CGH40010F 10 W GaN HEMT active device used for the proposed design. An extensive thank you to Keysight Technologies for donating a full license for Agilent Advanced Design Systems (ADS) which was fundamental to design procedure and extensively utilized.

VI. References

[1] M. J. F. Andrei Grebennikov, Switchmode RF and Microwave Power Amplifiers, Academic Press, 2021.

[2] D. G. M. Y. V. R. V. K. A. G. M. T. Moïse Safari Mugisho, "Generalized Class-E power amplifier with shunt capacitance and shunt filter," in *IEEE Transactions on Microwave Theory and Techniques*, 2019.

[3] F. G. E. L. Paolo Colantonio, High Efficiency RF and Microwave Solid State Power Amplifiers, Tor Vergata, Italy: John Wiley and Son's, Ltd, 2009.

[4] N. B. C. Jose Carlos Pedro, Intermodulation Distortion in Microwave and Wireless Circuits, Boston: Artech House, 2003.

[5] Z. Wang, Envelope Tracking Power Amplifiers for Wireless Communications, Artech House, 2014.

[6] J. L. Walker, The Handbook of RF and Microwave Power Amplifiers, Cambridge University Press, 2012.

[7] N. O. S. Andrei Grebennikov, Switchmode RF Power Amplifiers, Amsterdam: Newnes, 2007.

[8] S. D. MacPherson, An Introduction to High Frequency Small-Signal Amplifier Design, 2002.

[9] J. E. A.J. Wilkinson, "Transmission-Line Load-Network Topology for Class-E Power Amplifiers," in *IEEE Transactions on Microwave Theory and Techniques*, 2001.

[10] M. R. A. H. Roohollah Bameri, "A 2.4 GHz Class-E Power Amplifier with High Power Control Range," in *25th Iranian Conference on Electrical Engineering (lCEE20 17)*, 2017.

[11] V. A. B.-H. G. J. S. C. Qianqian Liu, "A Class-E RF Power Amplifier with a Novel Matching Network for High-Efficiency Dynamic Load Modulation," in *IEEE International Symposium on Circuits and Systems (ISCAS)*, 2017.

[12] C. S. D-A. Nguyen, "A high-efficiency design for 5-W 2.4/5.8 GHz concurrent dual-band class-E power amplifier," in *Microwave and optical technology letters, 2021, Vol.63 (4)*, 2021.

[13] I. L.-H. D. F.-R. J. L.-Y. M. M.-C. C. P.-W. E. H.-D. J. R.-H. P. M. D. Ochoa-Armas, "A nonlinear empirical I/V model for GaAs and GaN FETs suitable to design power amplifiers," in *International journal of RF and microwave computer-aided engineering, Vol.31 (3)*, 2021.

[14] H. H. A. Sheikhi, "Analysis and Design of the Novel Class-F/E Power Amplifier with Series Output Filter," in *IEEE Transactions on Circuits and Systems II, Express Briefs, Vol. 69, No. 3*, 2022.

[15] H. J. F. Moloudi, "Broadband class-E power amplifier design using tunable output matching network," in *International journal of electronics and communications, vol. 118*, 2020.

[16] T. A. Filipek, "Design and Optimization of High Efficiency GaN HEMT Class-E Power Amplifiers," in *TENCON 2015 - 2015 IEEE Region 10 Conference*, 2015.

[17] X. G. I. H. K. W. J.V. de Almeida, "High-Efficiency Moderate-Power Amplifier Using Packaged GaN Transistor With Improved Average PAE and Gain for Batteryless IoT Applications," in *IEEE transactions on microwave theory and techniques, Vol.71 (2)*, 2023.

[18] X. L. Y. Z. T. Q. X. D. W. C. F. G. C. Liu, "Investigation of High Efficiency Parallel Circuit Class-EF Power Amplifiers with Arbitrary Duty-Cycles," in *IEEE transactions on industrial electronics (1982), 2021, Vol.68 (6)*, 2021.

[19] S. C. Bera, Microwave High Power High Efficiency GaN Amplifiers for Communication, Springer Nature Singapore, 2022.

[20] J. L. K. A. R. W. P. K. S. A. D. L. T. Hwang, "Class-F Power Amplifier with 80.1% Maximum PAE at 2 GHz for Cellular Base-station Applications," in *IEEE Annual Conference on Wireless and Microwave Technology (WAMICON)*, 2013.

[21] S. G. S. H. S. I. L. U. K. M. a. R. A. Y. Hongtao Xu, "A High-Efficiency Class-E GaN HEMT Power Amplifier at 1.9 GHz," in *IEEE MICROWAVE AND WIRELESS COMPONENTS LETTERS, VOL. 16, NO. 1, JANUARY 2006*, 2006.

[22] A. B. V. F. Mury Thian, "High-Efficiency Harmonic-Peaking Class-EF Power Amplifiers With Enhanced Maximum Operating Frequency," in *IEEE TRANSACTIONS ON MICROWAVE THEORY AND TECHNIQUES, VOL. 63, NO. 2, FEBRUARY 2015*, 2015.

[23] R. N. a. F. M. G. Pouya Aflaki, "Design and implementation of an inverse class-F power amplifier with 79 % efficiency by using a switch-based active device model," in *2008 IEEE radio and wireless symposium [front matter]*, 2008.

[24] G. C. a. J. C. H. Kim, "A high-efficiency inverse class-F power high-efficiency inverse class-F power," in *Microw. Opt. Technol. Lett., vol. 50, no.*, 2008.